Ultrahigh Resolution Scanning
Electron Microscope
SU9000II

HITACHI
Inspire the Next

SU9000II

ULTRAHIGH-RESOLUTION SCANNING
ELECTRON MICROSCOPE

Science for
a better tomorrow

Science for a better tomorrow

Notice: For correct operation, follow the instruction manual when using the instrument.

Specifications in this catalog are subject to change with or without notice, as Hitachi High-Tech Corporation continues to develop the latest technologies and products for our customers.

Hitachi High-Tech Corporation

Tokyo, Japan
www.hitachi-hightech.com/global/en/products/microscopes/

HTD-E295 2023.5

Nanometer-scale morphology observation is critically needed due to the trend of miniaturization and high-level integration in semiconductor devices and development of advanced materials. In this regard, Hitachi High-Tech has been developing scanning electron microscopes (SEM) that enable sub-nanometer observations.
Since its release in 2011, the SU9000 incorporated Hitachi High-Tech's core competency technologies in pursuit of the key goal: ultrahigh-resolution observations with high throughput and stable operation. The SU9000 achieved the world's highest resolution*1 of 0.4 nm at 30 kV accelerating voltage through a large number of fundamental performance enhancements including a high-brightness electron gun and a low-aberration lens.
Now, Hitachi High-Tech announces the SU9000II, which can achieve a resolution of 0.7 nm even at 1.0 kV landing voltage (with deceleration feature option).
To allow for stable data acquisition at the instrument's highest performance levels, the SU9000II offers new capabilities that render automated adjustments of the optical system—and the new EM Flow Creator software package as an option to render automated data acquisition, particularly sequential data collection.
Hitachi High-Tech is proud to announce the SU9000II, a new in-lens SEM system for the forefront of development and evaluation of next-generation semiconductor devices and advanced functional materials.

Note: The system shown in the photograph is equipped with optional features. ＊1: As of May 2023

Key features

- Cold field-emission electron gun allowing both low energy spread and stable probe current at high brightness
- Ultrahigh vacuum specimen chamber further reducing contamination source
- High-rigidity frame and acoustic enclosure ensuring high-performance operation under a wide variety of environments

Cold field-emission electron source

Cold field-emission (FE) electron sources offer unparalleled capabilities for high-resolution observation. Hitachi High-Tech introduced the first commercial cold FE electron source in 1972 and has worked continuously to improve the technology ever since.
Instruments equipped with our latest electron guns can provide stable electron beam irradiation with a high-brightness.
In addition to enabling image acquisition with a high signal-to-noise ratio—even at low accelerating voltages—the SU9000II allows stable observations that require high probe current irradiation over a long period of time.

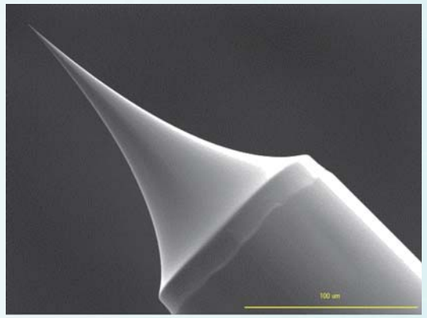

Cold field emitter tip

SEM electron sources: Performance comparison

	Cold FE electron source	Schottky electron source
Diameter (nm)	5	20
Energy spread (eV)	0.2～0.3	0.6 ～1.0
Brightness (A/cm^2/sr)	10^8	10^7

Low-aberration in-lens objective lens

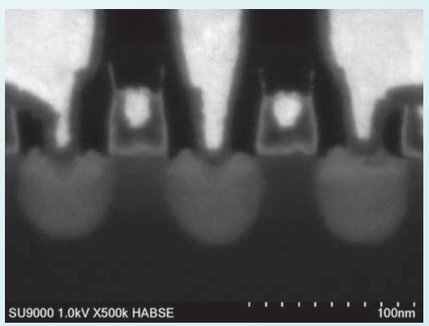

In-lens type objective lens has the advantage of reducing aberration by shortening the focal length. Reduced aberration can improve the resolution, allowing more stable observations for fine structures at the sub-10 nm scale or even below.
The figure on the left shows a backscattered-electron image of an ion-milled cross section of a PMOS transistor after cleaving.
The backscattered-electron signal clearly reveals information on the cross-sectional composition of the device, including the e-SiGe morphology.

Specimen: PMOS transistor
Backscattered electron image
Accelerating voltage: 1 kV
Magnification: 500 kX

Electron-optics and detector systems

SU9000II

- Cold FE electron source allows both high brightness and narrow energy spread.
- In-lens objective lens is the powerful tool for reducing aberration.
- Various detectors are utilized for detecting secondary-electron, backscattered-electron, and transmission-electron signals.

SU9000II: Schematic diagrams of electron-optics and detector systems

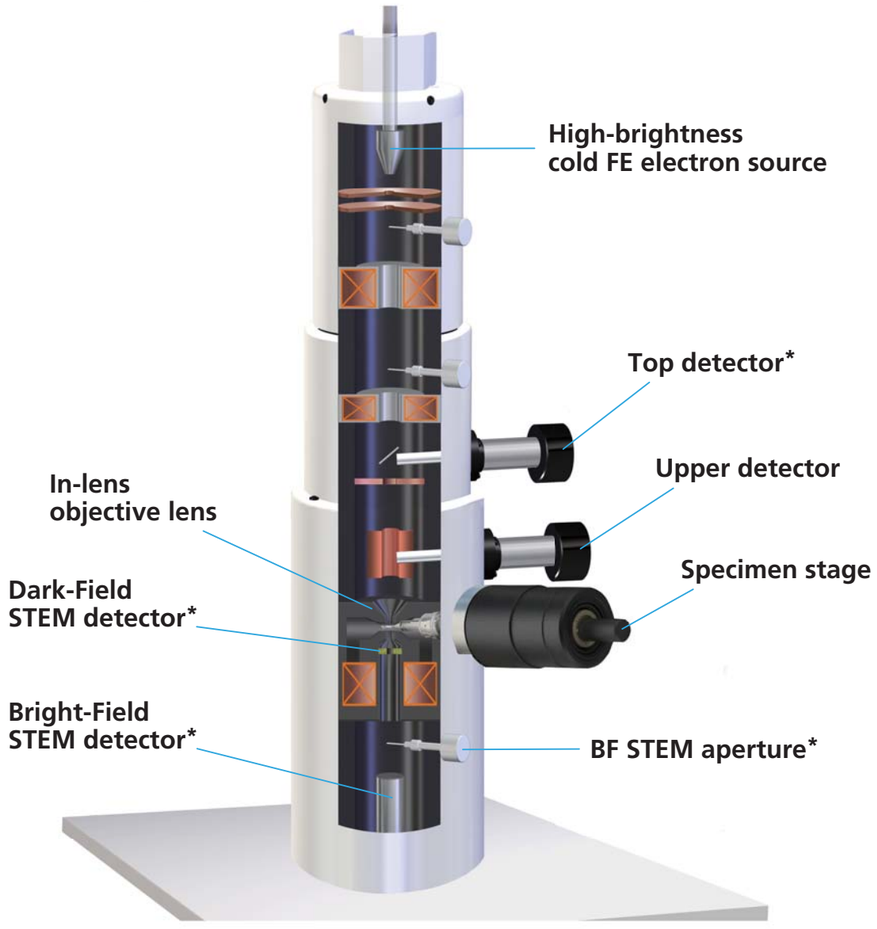

- Upper detector acquires secondary-electron signal or low-angle backscattered-electron signal.
- Top detector acquires primary high-angle backscattered-electron signal. Compositional contrast can be further enhanced with the energy filter function.
- A BF/DF Duo-STEM detector can be mounted to enable detection by discriminating the scattering angle of transmitted electrons.

Note: Asterisks indicate optional components.

Application in bulk specimens

Acquisition of multiple surface information of catalyst (gold/alumina carrier) specimen using top and upper detector.

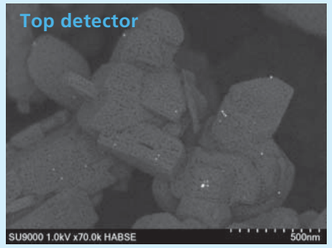

Compositional information provided by high- angle backscattered-electron signal highlights distribution of metal nanoparticles on specimen surface.

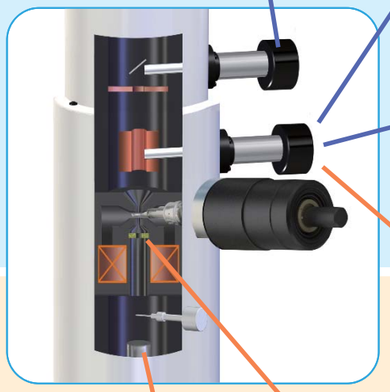

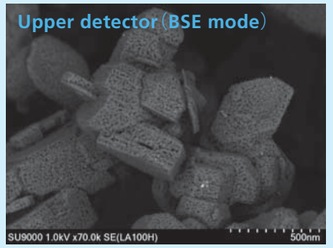

Composition and topography information provided by low-angle backscattered-electron signal allows visualization of pores in carriers.

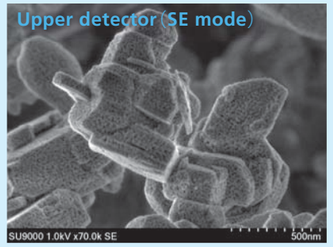

Secondary-electron signal allows visualization of surface microstructure.

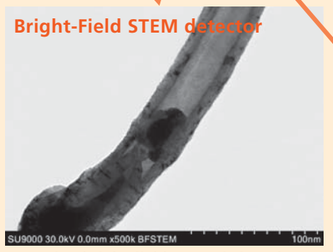

Detecting bright-field transmission-electron signal allows visualization of internal microstructure.

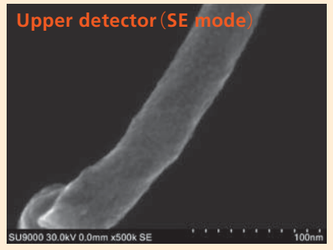

Secondary-electron signal allows visualization of microstructure on nanotube surface.

Application of nanomaterials and thin films

Simultaneous multiple signal collection of SE, BF-STEM, and DF-STEM signals was demonstrated in imaging of a multi-walled carbon nanotube.

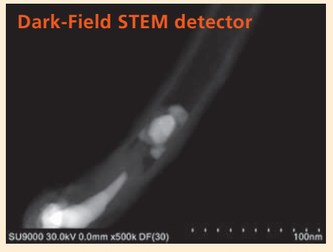

Detecting high-angle scattered transmission-electron signal allows visualization of the distribution of metal catalyst particles inside carbon nanotube.

Exploring new possibilities in LV STEM

Angle-selective Dark-Field STEM image

– BF/DF Duo-STEM detector* –

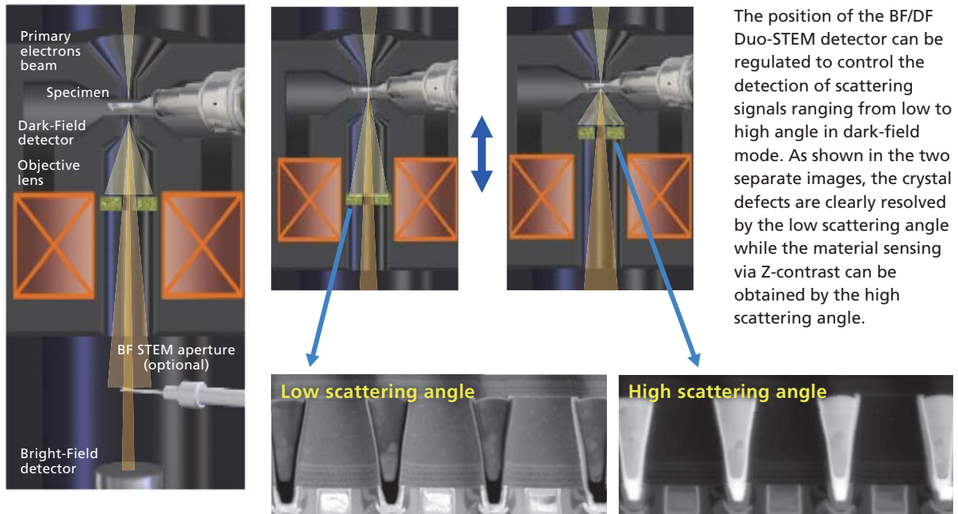

The position of the BF/DF Duo-STEM detector can be regulated to control the detection of scattering signals ranging from low to high angle in dark-field mode. As shown in the two separate images, the crystal defects are clearly resolved by the low scattering angle while the material sensing via Z-contrast can be obtained by the high scattering angle.

Specimen: NMOS transistor
Accelerating voltage: 30 kV

Lattice imaging by SEM/STEM

The SU9000II features a low-aberration in-lens objective lens and an optical system optimized for STEM observations. These features expand the range of available SEM/STEM observation techniques.
By controlling the convergence angle of the primary electron beam and generating interference fringes on the detection plane of transmitted electrons, lattice images can be observed in SEM/STEM.
The figure on the right shows a bright-field STEM image of pyrophyllite, revealing (020) plane lattice fringes with spacings of 0.445 nm.

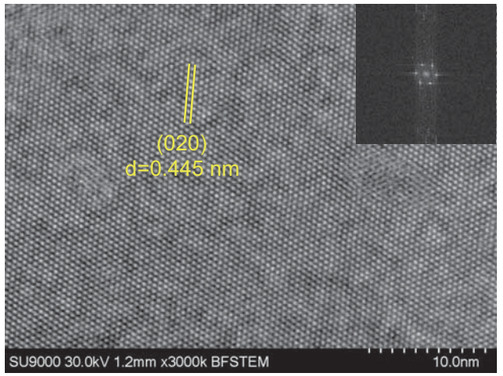

Specimen: Pyrophyllite
Accelerating voltage: 30 kV

Note: Asterisks indicate optional components.

SEM/STEM-based EELS analysis

EELS detector*

Diagram of SU9000II EELS detector

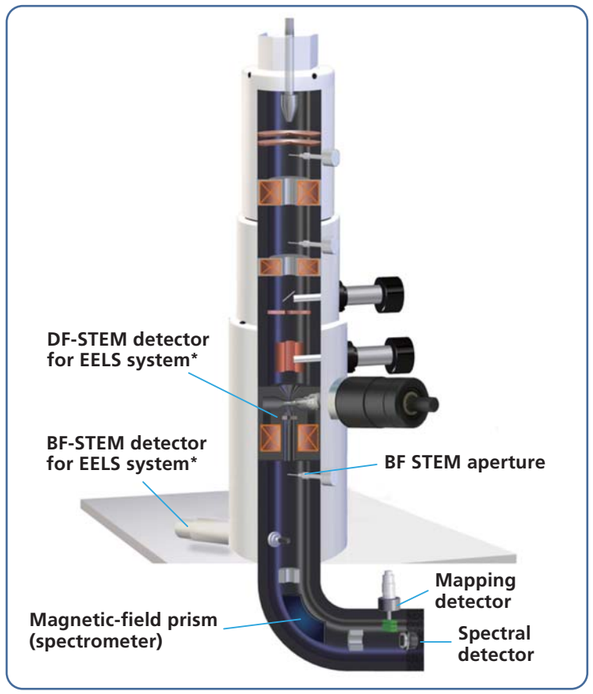

The SU9000II supports SEM/STEM-based electron energy-loss spectroscopy (EELS) analysis.
The EELS system disperses and collects the transmitted electron beam by a magnetic field prism and two detectors (serving either spectral or imaging application). It enables to acquire either spectral graphs or mapping related to the elemental composition and chemical bonding.

The detector unit consists of a spectral detector and a mapping detector with 3 sensors, allowing acquisition of elemental distribution images via the 3-window method using the mapping detector.

Both bright-field STEM image (left) and element mappings (upper right for Nitrogen, lower right for Oxygen) of the PMOS transistor region in a NAND flash-memory specimen are illustrated via approaches mentioned above.

Bright-field STEM image in NAND flash memory

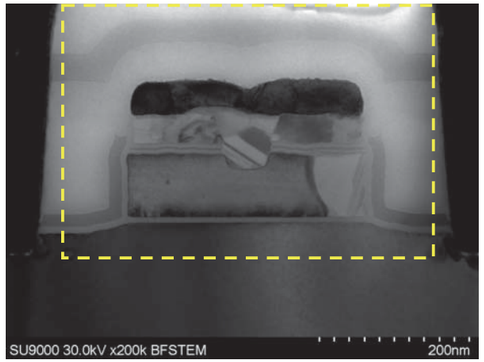

Specimen: NAND flash memory
Accelerating voltage: 30 kV
STEM image magnification: 200 kX

The BF/DF Duo-STEM detector can not be available with the EELS system.

EELS element mapping images

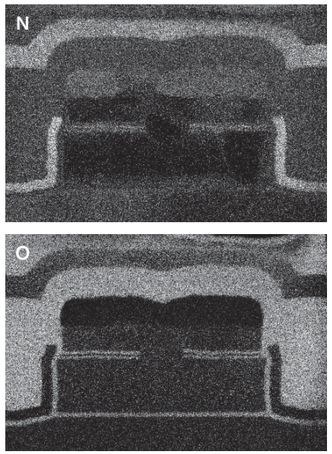

Note: Asterisks indicate optional components.

Photoresist: Morphology evaluation

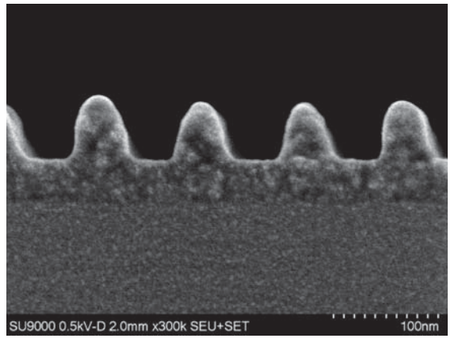

This example features a cross section of photoresist observed under low-energy conditions.
Applying a low accelerating voltage of just 0.5 kV allows clear imaging of the cross-sectional morphology of the photoresist while reducing damage to this vulnerable specimen by the irradiating electron beam.
The SU9000II can improve resolution under low-energy conditions by using the deceleration holder, which can be applied bias to the holder.
(Pt-coated.)

Plain view of DRAM capacitors: Morphology evaluation and compositional analysis

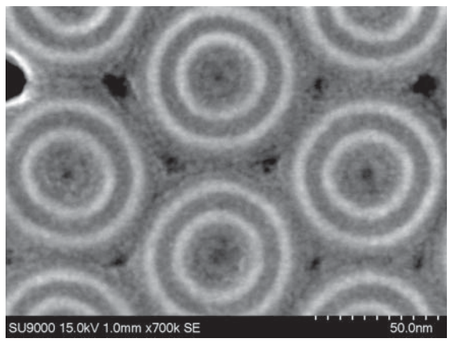

An example of a DRAM capacitor section exposed by ion milling.
In the upper left secondary electron image, concentric multi-layered structures of about 6 nm each can be seen inside the circular capacitor.
The figure at the lower left, the same sample was thinned and observed by STEM, and a multilayer structure ranging from layers of approximately 1 to several nanometers was clearly observed.
In the EDS elemental map image at the lower right, multiple layer structures with a width of 1 to 6 nm can be seen in the capacitor area, and each layer is composed of SiGe, TiN, ZrO_2 and other materials.

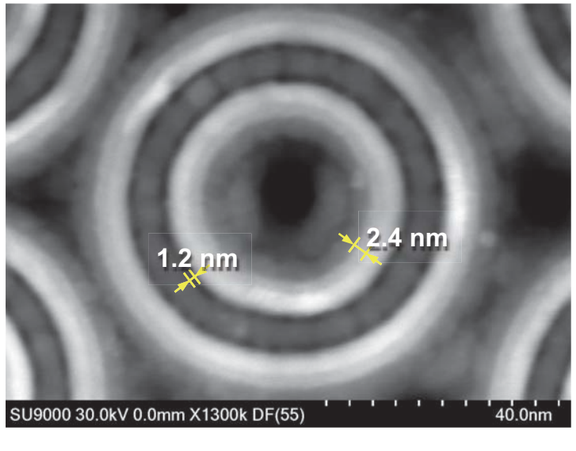

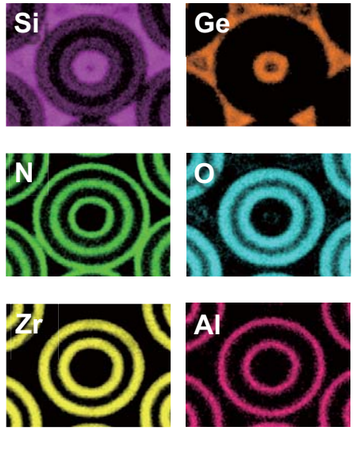

FinFET device: Morphology evaluation and compositional analysis

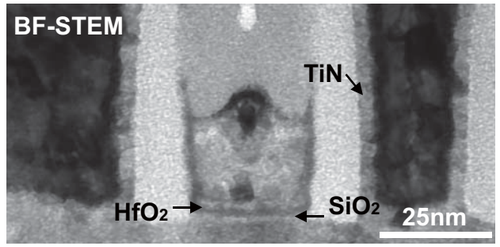

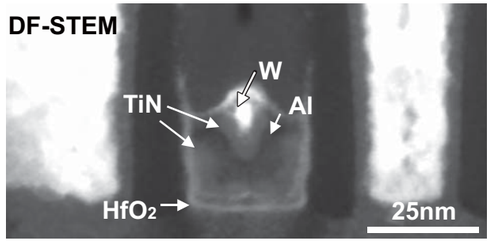

STEM image: magnification 1,200 kX
Accelerating voltage: 30 kV

A FinFET device morphology evaluation by STEM observation and composition- distribution analysis is performed by STEM/EDS.
The BF-STEM image (upper left) clearly distinguish the HfO_2 layer that is about 1.5 nm in thickness, as well as a TiN barrier-metal region with an approximate thickness of 3 nm. The DF-STEM image (lower left) shows composition contrast indicating the presence of various light metals near the metal gate; combining this information with the results of EDS quantitative mapping analysis (lower right) allows element distributions with nanometer-order resolution.

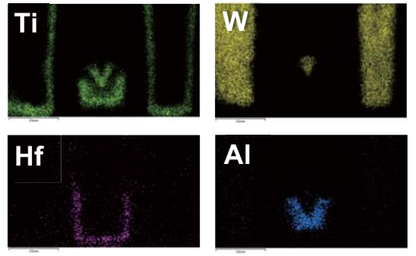

SiC MOSFET: Dopant distribution

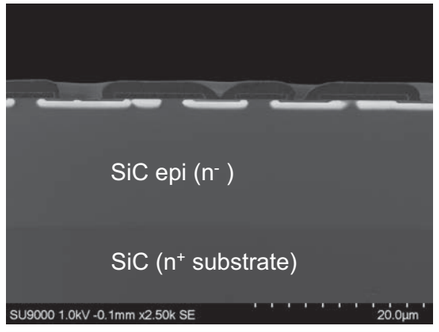

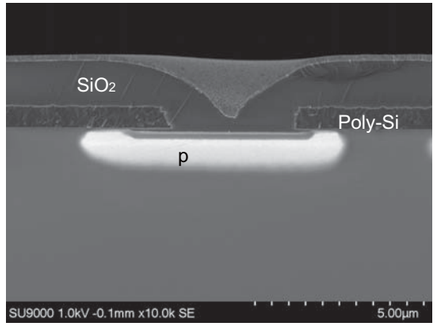

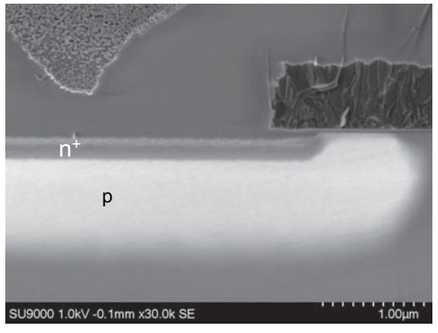

A SiC MOS FET cleaved cross section is observed at a low accelerating voltage of 1 kV to image dopant distribution.
In the upper-left image, the SiC substrate and the Epitaxial layer is identified by image contrast arising from the potential gap.
In the lower-left image, the p-dopant distribution inside the p-layer of a pn junction is discernible with high contrast. In the lower-right image—a further enlargement of the same field of view—the n^+ layer between the p-layer and the SiO_2 is visible.

Polymer-coated graphene: Evaluation of coating morphology

This example features observations of a graphene surface coated by an extremely thin polymer layer intended to serve as a carrier for gold nanoparticles.
As the polymer layer is an extremely thin film with a thickness of around 1 nm, the observation uses an ultra low landing voltage of 0.1 kV.
The region exposed graphene surface appears dark in the image due to the differing secondary-electron emission yield of the polymer material and the graphene.

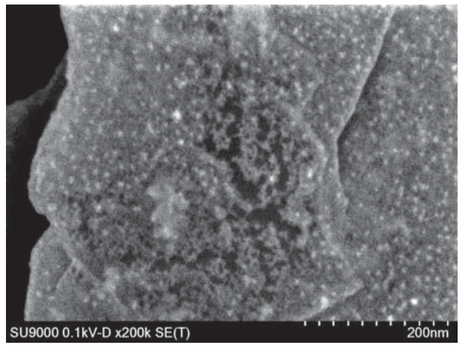

Schematic diagram of specimen

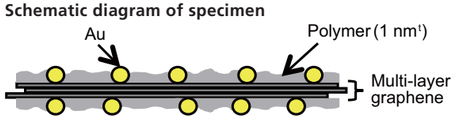

Specimen Courtesy of Professor Tsuyohiko Fujigaya, Associate Professor,
Applied Chemistry Department, Graduate School of Engineering, Kyushu University

Single-walled carbon nanotube: Distribution of catalyst fine particle

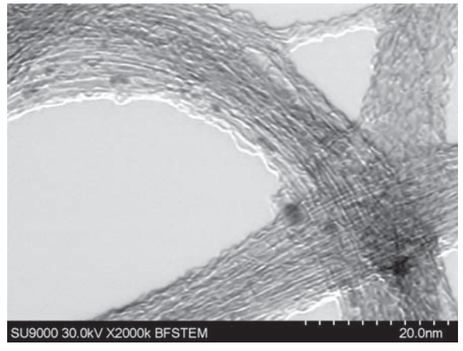

This example combines STEM observation of a single-walled carbon nanotube with EDS analysis of catalysts.
A STEM observation of the specimen at 2,000 kX magnification reveals residual catalyst particles with sizes of 1-5 nm in the dark-field STEM image. (Upper left: bright-field STEM image. Lower left: dark-field STEM image.)
EDS analysis confirmed the presence of Mo nanoparticles with sizes of 1-3 nm and Co nanoparticles with sizes of ~4 nm. (Lower right: EDS elemental mapping image)
The SU9000II can also provide high-resolution EDS analysis at a short working distance. Furthermore, it can render a wide-ranging collection of X-ray signals (with a high solid angle of 0.7 steradians). As a result, efficient identification of single-nanometer structures can be achieved in a short time.

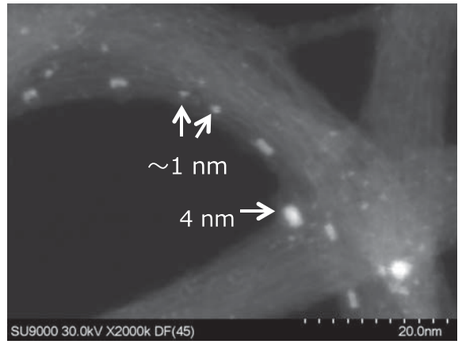

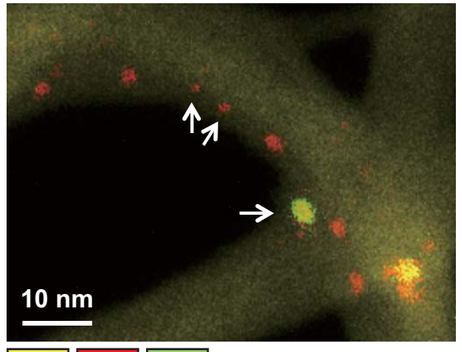

Multi-faceted evaluation of zeolite

Imaging of pores in artificially synthesized zeolite

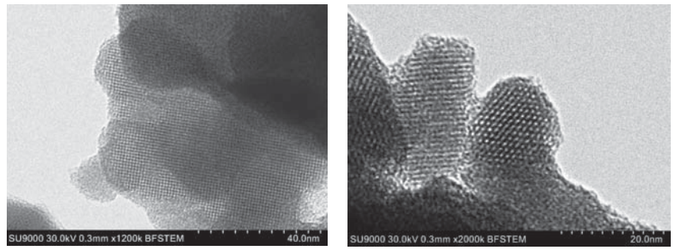

This example features STEM observation and characterization of pores in artificially synthesized zeolite (ZSM-5).
Left: Observation of ordered array structures.
Right: Image demonstrating that pore sizes are 1 nm or smaller.

STEM images:
Magnification 1,200 kX (left) or 2,000 kX (right);
Accelerating voltage: 30 kV

Coke analysis before and after catalytic reactions

– Cross-sectional observation and composition analysis of bulk specimens –

Cross-sectional zeolite after catalytic reactions

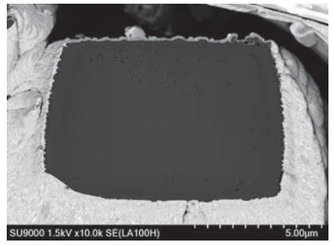

backscattered-electron image

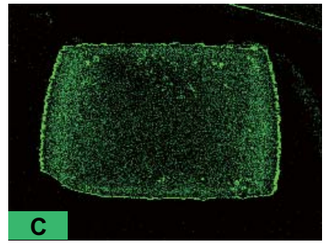

EDS/C mapping image

EDS mapping images of a cross-sectional zeolite after catalytic reactions show carbon—the principal component of coke—distributed over the surface and throughout the interior.

– STEM observation and EELS analysis of thin-filmed specimen –

Cross-sectional BF-STEM image of thin-filmed zeolite specimen

Shown in this case are the carbon K-edge excitation spectra acquired at both interfacial and interior regions of a thin-filmed zeolite particle. Peaks corresponding to various energies (283~335 eV) were captured. These spectra indicated the difference of chemical boning between interfacial and interior regions. This example illustrates the extended capabilities of the SU9000II, which can offer versatile characterizations ranging from elemental mapping in bulk states to identification of chemical nature in thin film specimen.

STEM image: Magnification 35 kX
Accelerating voltage: 30 kV

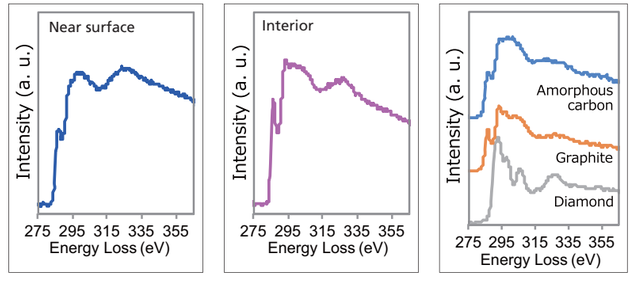

Energy-loss spectra obtained at observation points near surface and interior.
(Observation points indicated by color-coded circles in STEM image.)

Reference: EELS spectra of various forms of carbon

Specimen Courtesy of:
Mr. Toshiyuki Yokoi,
Tokyo Institute of Technology

Novel Coronavirus Image

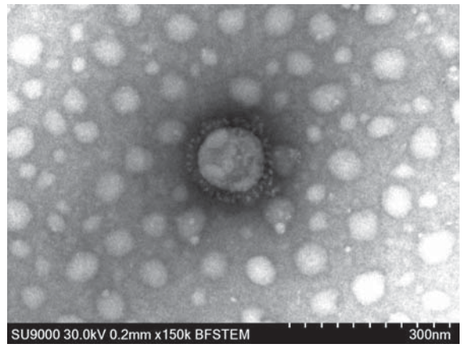

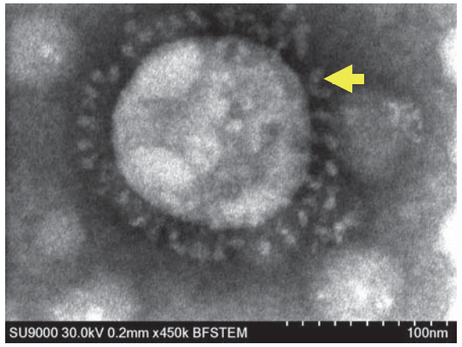

This is a STEM image of a negatively stained novel coronavirus.
From the image on the left, it is determined that the diameter is around 150 nm.
In the enlarged image on the right, the detailed shapes of the spike proteins (arrow) that are the receptor binding sites are clearly visible.

STEM image magnification: 150 kX (left), 450 kX (right);
Acceleration voltage: 30 kV

Influenza Virus Image

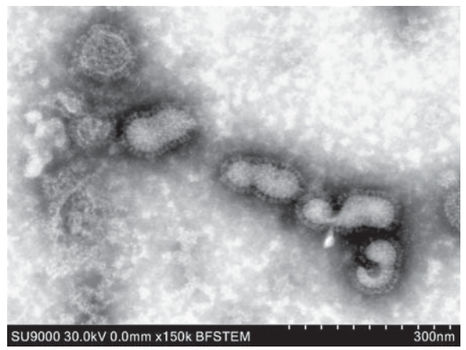

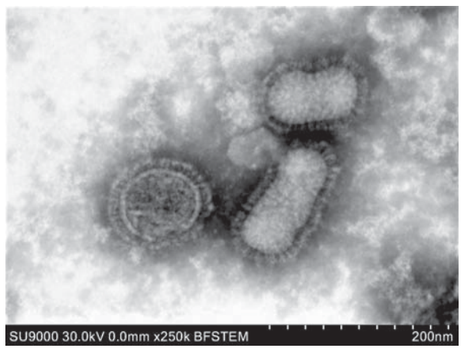

This is a STEM image of a negatively stained influenza virus.
The surface-spike structure is clearly visible.

STEM image magnification: 150 kX (left), 250 kX (right);
Acceleration voltage: 30 kV

Samples Courtesy of NBC Meshtec Inc.

Mouse Cardiomyocyte Section Image

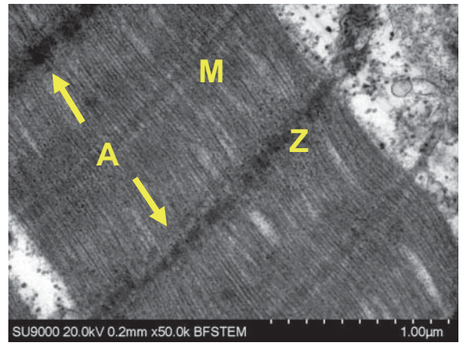

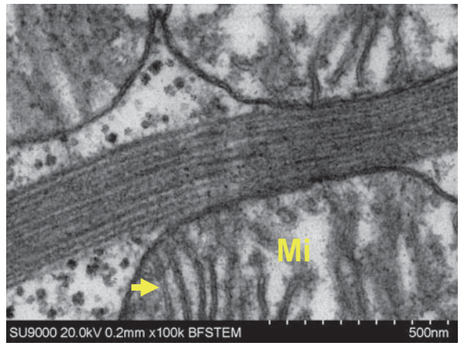

This is a STEM image of a mouse cardiomyocyte section.
In the image on the left, the cardiac muscle sarcomere structure is clearly visible, and the A band and the M and Z lines can be seen.
In the image on the right, the double membrane structure of the crista (arrow) of mitochondria distributed between the myofibrillar bundles is clearly visible.

STEM image magnification: 50 kX (left), 100 kX (right);
Acceleration voltage: 20 kV

Image of a Bacterium

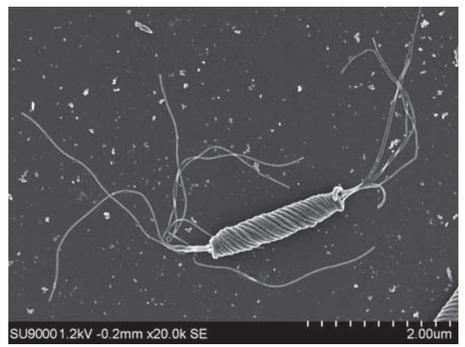

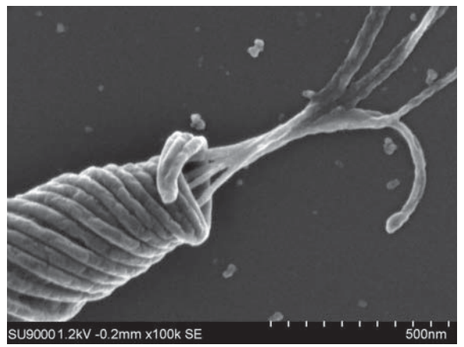

This is a low-voltage SEM image of a *Helicobacter bilis.*
In addition to the structure of the bacterium, the flagella and twisted forms thereof are visible.

SEM image magnification: 20 kX (left), 100 kX (right);
Acceleration voltage: 1.2 kV

Samples courtesy of Professor Yoshiaki Kawamura of the Aichi Gakuin University School of Pharmacy

Facilitating stable data acquisition SU9000II

Improving image clarity:

Real-time image acquisition capabilities*

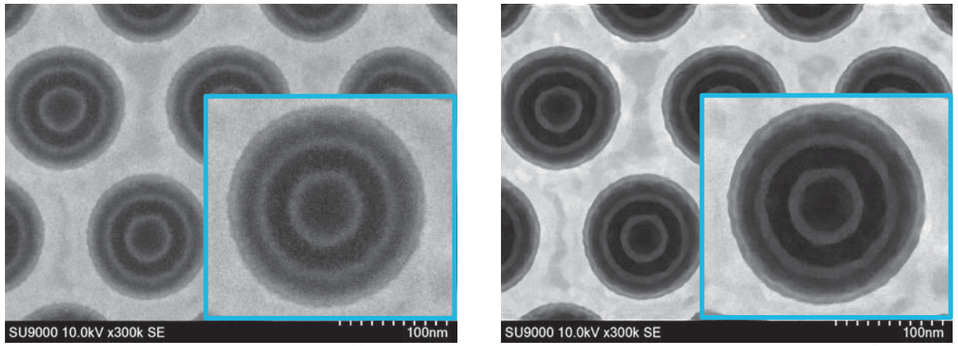

Unprocessed　　Processed

SU9000II can offer noise reduction and various other types of image processing in real time.
For example, edge enhancement effect shown in the image on the right leads to the facilitated further emphasize of the interfacial structures.
Image-processing features can be applied to both live images and captured images.

Note: Asterisks indicate optional components.

Streamlining automated data acquisition

Automated adjustment of electron-optics system

SEM observations require adjustments of settings and parameters depending on both the nature of specimens and the objectives of measurements.
The SU9000II features a high level of ease of use via providing a wide variety of automated operations such as focusing, astigmatism correction, brightness/contrast adjustments, as well as beam/aperture/astigmatism corrector alignments, etc.

EM Flow Creator*

"EM Flow Creator" allows users to configure repeatable SEM operation sequences.
Various SEM functions can be added assembled in EM Flow Creator's window by the drag-and-drop method and then by saving as a recipe for later use.
Once a recipe is configured, automated data collection under the set conditions can be performed with high accuracy and repeatability.
This minimizes the effort associated to capture images at many sample points or to make other measurements requiring extensive manual operation.

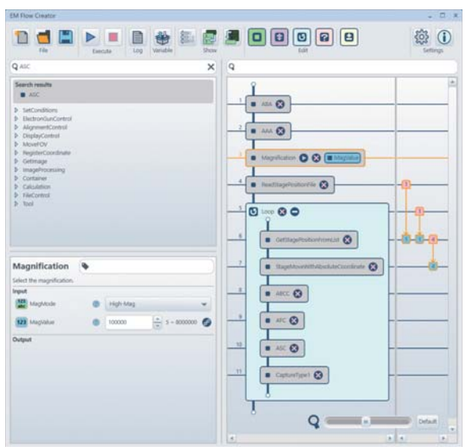

EM Flow Creator recipe creation image

Note: Asterisks indicate optional components.

Primary instrument specifications SU9000II

Specifications

Items		Description
SE image resolution		0.4 nm (Accelerating voltage : 30 kV)
		1.0 nm (Accelerating voltage : 1 kV)
		0.7 nm (Landing voltage : 1 kV*1)
STEM image resolution*3		0.34 nm (Accelerating voltage : 30 kV, Lattice image)
Accelerating voltage		0.5 to 30 kV
Landing voltage*1		0.1 to 2 kV
Electrical image sift		±5 µm (Sample Height = 0.0 mm)
Stage traverse		X : ±4.0 mm, Y : ±2.0 mm, Z : ±0.3 mm, T : ±40 °
Specimen Size	Flat specimen stage	5.0 mm × 9.5 mm × 3.5 mm (H) (Max.)
	Cross section specimen stage	2.0 mm × 6.5 mm × 5.0 mm (H) (Max.)
	Dedicated holder*3	Cross section specimen holder : 2.0 mm×12.0 mm×6.0 mm (H)
		Double tilt cross section specimen holder : 0.8 mm×8.5 mm×5.5 mm (H)

System Function

Items		Description
Magnification	LM Mode*2	80 to 10,000 x
	HM Mode*2	800 to 3,000,000 x
Electron optics	Beam blanking	Electrostatic type (synchronized with scanning signal)
Image display	Full screen display	1,280 x 960 pixels
	Single or Dual screen display	800×600 pixels / 800×600 pixels × 2
	Quad screen display	640 × 480 pixels × 4
	Image data saving	640 × 480, 1,280 × 960, 2,560 × 1,920, 5,120 × 3,840 pixels
	Saved image data management	SEM data manager (image database / image processing function) included

System Configuration

Items		Description
Electron optics	Electron gun	Cold cathode field emission source
	Lens system	3-stage electromagnetic lens reduction
	Objective lens aperture	Movable aperture (heating type. 4 openings selectable from outside of vacuum with fine adjustment)
Stage	Stage	Side entry goniometer stage
	Specimen holder	Standard holder (1 included)
	Specimen stage	6 types (1 included)
Detector	Detector	Secondary electron detector
		Top detector*3
		BF/DF Duo-STEM detector*3
		Energy dispersive X-ray detector*3
		EELS detector*3
Display system	OS	Windows®10*4
	Monitor	24.1 type wide screen LCD (subject to change without notice) (1,920×1,200)
	Operation system	Mouse, Keyboard, Rotary Knob, Stage controller (Trackball and Joystick combined)

∗1: With optional deceleration holder and top detector.
∗2: Magnification is specified with 127mm x 95mm (4 x 5 photo size) as the display size
∗3: Option
∗4: Windows® is a registered trademark of Microsoft Corp. in the USA and in other countries.
∗5: In case of connection from installation site facilities.
∗6: Assuming water vessel is empty.
∗7: Customer-supplied item.

Installation condition

Items	Description
Room temperature	15 to 25 ℃
Humidity	60 % RH or less (non-condensing)
Power (Main unit)	5 kVA (crimp contact for M6) AC100 V±10 %, or AC200-240 V ±10 % with autotransformer
Grounding	100 Ω or less
Cooling water(Chiller)	Dedicated Cooling Water Circulation system*7
water flow	0.6 to 1.0 l/min
pressure	50 to 100 kPa
temperature	15 to 20 ℃ (allowable fluctuations 0.5 ℃ /10min or less)
Supply faucet	Rc3/8 tapered female thread x1
Drain port	(20 mm dia. or more) x1 (Natural drain type located on floor)
Air Compressor	400 to 500 kPa (Rc1/4 tapered female thread)

Dimensions and weight

Items	Width (mm)	Depth (mm)	Height (mm)	Weight (kg)
Main unit	1,140	1,310	1,860	946
Display unit	1,110	1,170	750	251
Power supply unit	670	690	1,380	230
Dry pump*7	260	400	340	25
Air compressor*7	240	420	520	16
Weight	200	320	180	25
Water circulator*7	380	550	620	50*6

Other special-purpose accessories

Dry pump / Air compressor / Anti-contamination trap / STEM holder / Autotransformer / Faraday cup / Video amplifier unit / Photomultiplier Power supply unit

Installation diagram